Electrolyte contact changes nano-$Li_4Ti_5O_{12}$ bulk properties – surface polarons enable Li^+ equilibrium between bulk and electrolyte

P. Philipp M. Schleker*[1], Cristina Grosu[1,2], Marc Paulus[1,3], Peter Jakes[1,3], Robert Schlögl[4], Rüdiger-A. Eichel[1,3], Christoph Scheurer[1,4], Josef Granwehr[1,5]

1 Institut für Grundlagen der Elektrochemie IEK-9, Forschungszentrum Jülich, Wilhelm-Johnen Straße, 52425 Jülich, Germany

2 Institut für Chemie, Technische Universität München, 85748 Garching b. München, Germany

3 Institut für Physikalische Chemie (IPC), RWTH Aachen University, D-52074 Aachen, Germany

4 Fritz-Haber-Institut der Max-Planck-Gesellschaft Faradayweg 4–6, 14195 Berlin, Germany

5 Institut für Technische und Makromolekulare Chemie (ITMC), RWTH Aachen University, D-52074 Aachen, Germany

e-mail: p.schleker@fz-juelich.de

Abstract: It is of general interest to combine the faradaic processes based high energy density of a battery with the non-faradaic processes based high power density of a capacitor in one cell. Surface area and functional groups of electrode materials strongly affect these properties, but a mechanistic explanation for the interplay between such process and how to balance them is largely missing. For the anode material $Li_4Ti_5O_{12}$ (LTO), we suggest a polaron based mechanism that influences Li ion uptake and mobility. Electrolytes containing a lithium salt induce an observable change in the bulk NMR relaxation properties of LTO nano particles. The longitudinal ^{7}Li NMR relaxation time of bulk LTO can change by almost an order of magnitude and, therefore, reacts very sensitively to the cation and its concentration in the surrounding electrolyte. The reversible effect is largely independent of the used anions and of potential anion decomposition products. It is concluded that lithium salt containing electrolytes increase the mobility of surface polarons. These polarons and additional lithium cations from the electrolyte can now diffuse through the bulk, induce the observed enhanced relaxation rate and enable the non-faradaic process. This picture of a Li^+ ion equilibrium between electrolyte and solid may help with improving the charging properties of electrode materials.

Introduction

Energy storage systems are essential for a broad range of applications with requirements as diverse as powering a continuously increasing number of portable devices, as traction power sources in electrically powered vehicles, or to stabilize the power level in electricity networks. Therefore, industrially viable materials for energy storage systems need to be adapted to various use cases[1], which requires detailed mechanistic understanding of underlying processes in batteries and capacitors[2-3]. The energy density and the power density are two essential parameters, the former describing the amount of energy that can be stored and the latter how quickly this energy can be stored or released. Very generally, the distinction can be made between faradaic electrochemical processes such as intercalation of ions into the material, which are slow but allow for a high energy density, and non-faradaic physical processes such as double layer formation, which are fast and, therefore, facilitate a high power density. Faradaic processes are intensively studied in the context of battery materials, but the origin of their non-faradaic processes contribution, which can be dominant in high surface materials, is still unclear. It was summarized that “for the further advancement of electrical energy storage” systems “the influence of the surface chemistry on the electrochemical properties of materials” needs to be understood.[4] The interplay between surface and bulk in sense of faradaic and non-faradaic processes are therefore of broad interest.

In general the characterization of pristine materials for batteries is of importance to understand their fundamental properties [5-6]. These properties can be tuned by several strategies, like doping with other atoms, by particle size adaption, and by modification of the surface structure. The last two approaches effected different bulk properties for the same bulk material.[7] Therefore the cycling behavior and rate capability in batteries are commonly tested to correlate changes of surface and particle size with changes in the performance.[8]

It is well accepted that surface processes play a crucial role for the properties and performance of batteries and capacitors, yet there are still large gaps in our understanding of the relevant mechanisms.[4] TiO_2, for example, is an important, much studied material[9] that exhibits faradaic and non-faradaic properties, which both depend on particle size and manufacturing process[10]. There seems to be a dynamic dependence between the observed bulk characteristics of active materials and the nature of their surface.[11] Surface modification dependent changes in a bulk material are difficult to observe. A publication by Lee *et al.* reported on a direct observable examples of a strong conductivity change in bulk AgX caused by surface modification with Al_2O_3.[12]

Compounds from the binary LiO_2–TiO_2 composition line such as $Li_4Ti_5O_{12}$ (LTO), for example, have shown both very good cycling stability and very high rate capability[13-14]. On the other hand, Li ion mobility in stoichiometric LTO appears to be low[15], yet strongly morphology dependent, with nanostructured LTO showing considerably faster Li ion dynamics[16]. Furthermore, the addition of small amounts of lithium cause the resulting $Li_{4+X}Ti_5O_{12}$ to be a fast conducting material.[15, 17-19] Other publications on the diffusion of Li^+ in

rutil[20-21] and LTO[22] support the idea of polaron hopping. Polarons are, in a simplified picture, mobile negatively charged quasi-particles with an ionic bond portion.[23] For LTO, recently developed simulation techniques were able to show that polarons are more stable at the surface than in the bulk.[24]
However, as soon as a material is inserted into an electrochemical cell for testing, a multitude of additional processes occur, which hinders the individual investigation of specific mechanisms. Here, dry LTO is compared to LTO in contact with different electrolytes to analyze potential effects on bulk properties of the solid material. It is investigated whether, in principle, chemical surface reactions are induced, and if these changes affect the Li ion mobility. Nuclear magnetic resonance (NMR) relaxation is used to identify changes of the dynamics in the material. By employing Laplace inversion of the data, fractional differences in relaxation behavior due to Li mobility in different sample environments can be identified without *a priori* assumptions regarding the number of individual components. Thereby, it would be possible to distinguish between core–shell relaxation behavior if a surface layer changes its properties, and bulk effects if changes on the surface have a long-range impact on the physical properties of the material.

Results

Commercial battery grade nano-LTO powder was brought in contact with different electrolytes containing ether lithium or sodium as cations and PF_6^-, Triflate (Tfl^-) or Tetrakis-(pentafluorophenyl)-borate (Tpb^-) as anions (Figure 1). The longitudinal relaxation time constant T_1 of bulk ^{7}Li nuclei was recorded in a temperature range from -10°C to 50°C. We inverted the recorded data using Inverse Laplace Transformation (ILT) without non-negativity constrains.[25] By this it is possible to separate relaxation processes in solid lithium conducting materials.[26-28]

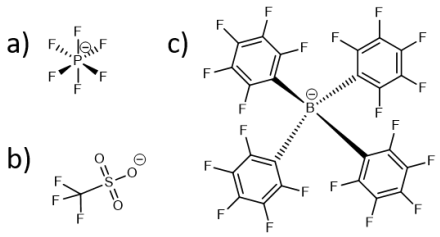

Figure 1: The three anions used in this study. a) PF_6^-, b) Tfl^-, c) Tpb^-

The procedure is exemplified on pure LTO under Argon atmosphere (Figure 2). The first row shows static ^{7}Li NMR spectra of the sample measured at -10°C, 20°C and 50°C. The blue spectrum is the fast relaxing contribution to the overall spectrum, calculated as the sum of the relaxation distribution between 25s and 80s, and the red spectrum is the slowly relaxing contribution to the spectrum between 100s and 315s. The second row shows the spectrally resolved T_1 distribution of the three measurements. The third row compares the T_1 distribution of the three temperatures, integrated along the spectral dimension. It is evident that the temperature has a small but observable effect on the maximum and the distribution of the T_1 relaxation. While the exact distribution may vary slightly due to the ill-posedness of the problem, the mean, the median or the width of each mode are quite robust parameters.[29] Hence, the position of the maximum and the mean are used to analyze the effects of the solvents and temperature in the following.

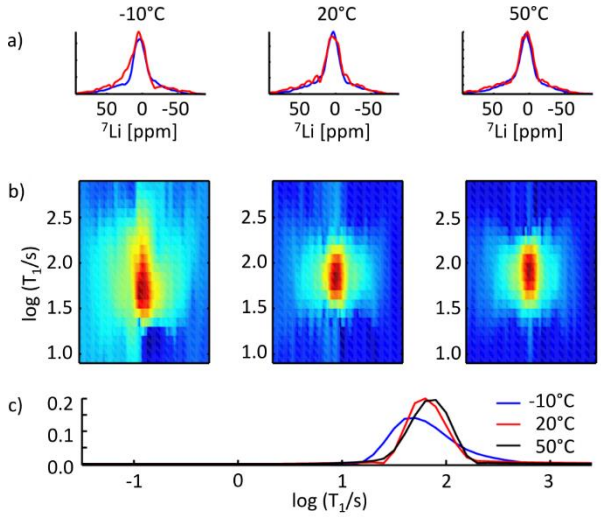

Figure 2: Principle of data analysis for static ^{7}Li NMR T_1 measurements of nano-LTO powder at -10°C, 20°C and 50°C using Inverse Laplace Transformation with non-negativity constrains. a) Spectral density integrated between 25s and 80s (blue line), and between 100s and 315s (red line), scaled by a factor 3. b) Spectrally resolved distribution of ^{7}Li NMR T_1 relaxation time distribution. c) T_1 relaxation time distribution of ^{7}Li, integrated over the spectral dimension.

We prepared a series of 8 different samples (Figure 3). The results of the ILT for four samples measured at 10°C and 30°C is given exemplary in Figure 3a. A pink box is drawn as guide for the eye. It marks the upper and lower T_1 relaxation values for the LTO in EC/DMC at 30°C as reference (Figure 3a, first row). The use of 1 M $LiPF_6$ (Figure 3a, second row) and 2 M $LiPF_6$ (Figure 3a, third row) result in a reduction of the bulk relaxation. The use of 1 M NaTfl (Figure 3a, last row) shows the opposite effect. It is noteworthy that the lithium containing electrolytes cause an additional liquid-state ^{7}Li NMR signal with a relaxation time of about 2s. It originates from solvated Li^+ in the electrolyte and can easily be separated in the relaxation time dimension. However, subtraction of this feature by using the pure electrolyte is not straightforward since weak features, most probably caused by Li ion exchange between electrolyte and LTO, lead to spectrally narrow signal components at relaxation times of Li ions in the solid. This is expected if Li ions exchange between the inversion pulse and the detection pulse, hence relax during part of the recovery delay in one environment and are detected in the other.

We extract from these results in the aforementioned way the maxima distribution (Figure 3b) and the mean distribution (Figure 3c) of the T_1 relaxation of each sample at a given temperature.

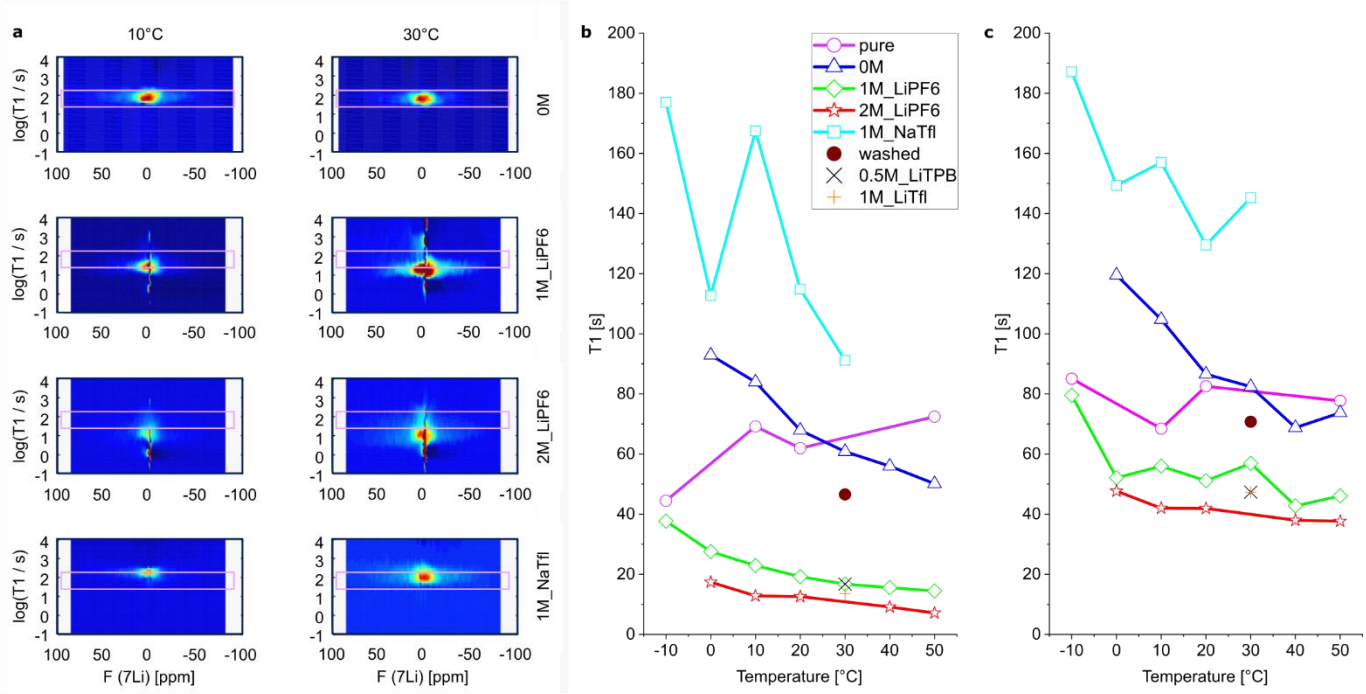

Figure 3: a) exemplary T_1 relaxation distribution of ^{7}Li in 4 different samples measured at 10°C and 30°C b) Position of maxima and c) mean distribution of T_1 relaxation of ^{7}Li in all 8 LTO samples with changing electrolyte. No electrolyte (pink circle, pure), organic solvent without salt (blue triangle, 0M), 1 M $LiPF_6$ electrolyte (green diamonds, 1M_LiPF6), 2 M $LiPF_6$ electrolyte (red stars, 2M_LiPF6), 1 M $NaSO_3CF_3$ (cyan squares, NaTfl), 1M sample washed and measured with organic solvent without salt (brown dot, washed), 0.5 M $LiC_{24}BF_{20}$ (black X, 0.5M_LiTPB), 1 M $LiSO_3CF$ (orange cross, 1M_LiTfl)

Pure LTO under Argon atmosphere (Figure 3 b,c, pink circles) shows at -10°C the lowest value in the T_1 maxima distribution at 44.5s and a highest value of 72.4s at 50°C. It is the only sample, where the maximum of relaxation time rises with increasing temperature. The Mean distribution stays quite constant between 70s and 85s for the same sample (Figure 3b, c, pink circles). Such a convergence of the maximum and mean indicates that the relaxation mode becomes more symmetric at increased temperatures, which can also be observed in Figure 2c.

The contact with an organic solvent consisting of dimethylcarbonate and ethylcarbonate (1:1 by volume), henceforth called electrolyte, without salt (0M, blue triangles, Figure 3b,c) resulted at 20°C in similar relaxation behavior as the dry material. It shows a change in the slope of the temperature dependence of the maximum distribution and the mean distribution. For both distributions of the 0M sample an increase in temperature results in a decrease in relaxation time (blue line, Figure 3). Yet the effect is weak and will not be further discussed.

We used a 1 M $LiPF_6$ (1M_LiPF6, green diamonds, Figure 3b, c) solution with the same organic solvent as next eluent. It resulted in a significant reduction of the T_1 relaxation time of the bulk ^{7}Li signal for all temperatures. The maximum of the T_1 relaxation time distribution at 30°C drops from 60.8s in 0M to 16.7s in 1M_LiPF6 sample, while the mean value drops from 82.4s to 56.9s. This is a general trend for all temperatures. The effect increases when going to a 2M $LiPF_6$ solution (2M, red stars, Figure 3). The relaxation time value at 30°C is 10s for the maximum and 40s for the mean value.

Such a strong relaxation effect, which affects the whole T_1 distribution of ^{7}Li in LTO, is only plausible if Li in the LTO bulk is affected by a changing mobility or an altered strength of interactions responsible for relaxation, such as additional paramagnetic centers in the bulk. Additional mobile electrons in the bulk material could explain it. But their origin needs to be further addressed. Wilkening e.g. showed that the small amount of additional lithium ($Li^+ + e^-$) in $Li_{4.1}Ti_5O_{12}$ caused a tremendous reduction in T_1 relaxation time of ^{7}Li and with this an increased mobility of lithium ions, due to more mobile electrons in the bulk material[15].

To check whether the PF_6^- anion has specific properties that cause this effect, we compared the results with LiTfl and LiTpb, which are two chemically very different electrolyte salts with non-coordinating anions (Figure 1). All three anions are very weakly coordinating and have only the fluorine as element in common. Still the effect on the ^{7}Li relaxation time was reproducible and seems therefore to be independent of the used anion (Figure 3b,c black X and orange cross).

To further assure this effect is not induced by an irreversible surface modification e.g. due to the introduction of fluorine, we decantively washed the 1M sample of $LiPF_6$ four times with the salt-free organic solvent. The resulting sample (washed, brown dot, Figure 3) had strongly elongated relaxation time, close to the 0M sample. It shows the effect is at least to a major part reversible and, therefore, excludes irreversible surface modifications on the LTO nano particles to be responsible.[30] Any additional mobile negative charges must therefore be from LTO itself.

To investigate the role of the lithium cation we measured a 1M solution of sodium triflate (NaTfl, bright blue line, Figure 3) between -10°C and 30°C. Since sodium cannot intercalate into LTO. The mean of the relaxation time distribution increased at least by 20 seconds, which again can only be explained if relaxation of Li ions in the bulk of LTO is affected. The maxima of the relaxation show a larger deviation around the trend line, which is caused by the logarithmic sampling of the relaxation times during measurement. Nevertheless, one can adjust the maximum bulk relaxation time T_1 in those LTO nanoparticles within one order of magnitude using lithium or sodium containing electrolytes.
In the electrolyte free lithium cations could be observed, which are probably caused by a partial exchange of Li with Na in LTO. Such an exchange could lead to a stronger shifting of polarons to the LTO surface. Since Na is restricted to the LTO surface only, initially bulk polarons, which enable the mobility of lithium cations in the bulk, now lead to a reduced influence on the bulk relaxation time T_1. With lithium containing electrolytes lithium ions from the solution diffuse into the bulk material, acquiring polarons from the surface.

Discussion

From these results we can conclude on the equilibria in the "three phase system" of LTO bulk, LTO surface and electrolyte (Figure 4). There are three cases to be summarized. First, an organic solvent has only a marginal effect on the equilibrium between surface and bulk. It leaves the equilibrium from that point of view untouched (Figure 4b). Second, a sodium containing electrolyte causes a shift of the mobile polarons from the bulk to the surface, as mobile lithium ions can exchange with sodium ions from the electrolyte. As the mobility of lithium in LTO is correlated with a mobile polaron, this negative charge is now pinned to sodium on the surface. (Figure 4a). Finally a lithium containing electrolyte will cause a shift of polaron concentration from the surface into the bulk (Figure 4c). Excess lithium cations from the solvent can diffuse into the bulk and drag the polarons due to charge neutrality in bulk with them. The Anions should only have a minor influence on this polaron concentration shift. They are very weakly coordinating, and in case of Tpb^- the negative charge is sterically very well shielded.

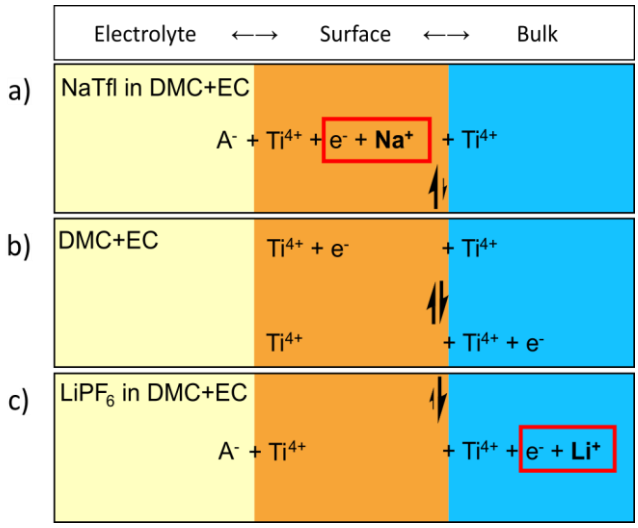

Figure 4: Equilibria between electrolyte, surface and bulk of LTO. A) Sodium cations interact with the surface and shift polarons to it. b) The electrolyte DMC/EC has no effect on the surface-bulk equilibrium. c) Lithium cations from the electrolyte can diffuse with the surface polarons into the bulk.

This last point of charge neutrality is very important for a complete picture of the equilibrium between solid and electrolyte. The overall LTO nano-particles are not charged when in contact with the pure organic solvent. The lithium containing electrolyte causes additional positive charge carriers into the material by inserting lithium cations. Their positive charges are compensated in the bulk by the mobile polarons. The introduced positive charge are compensated by the anions, which form a layer close to the defects or vacancies on the LTO surface, leading to a solid electrolyte double layer (Figure 5). This fits to the observation of adsorbed $LiPF_6$ salts on soaked LTO electrodes[30] and could contribute to the discussion about SEI formation on LTO[31-36].

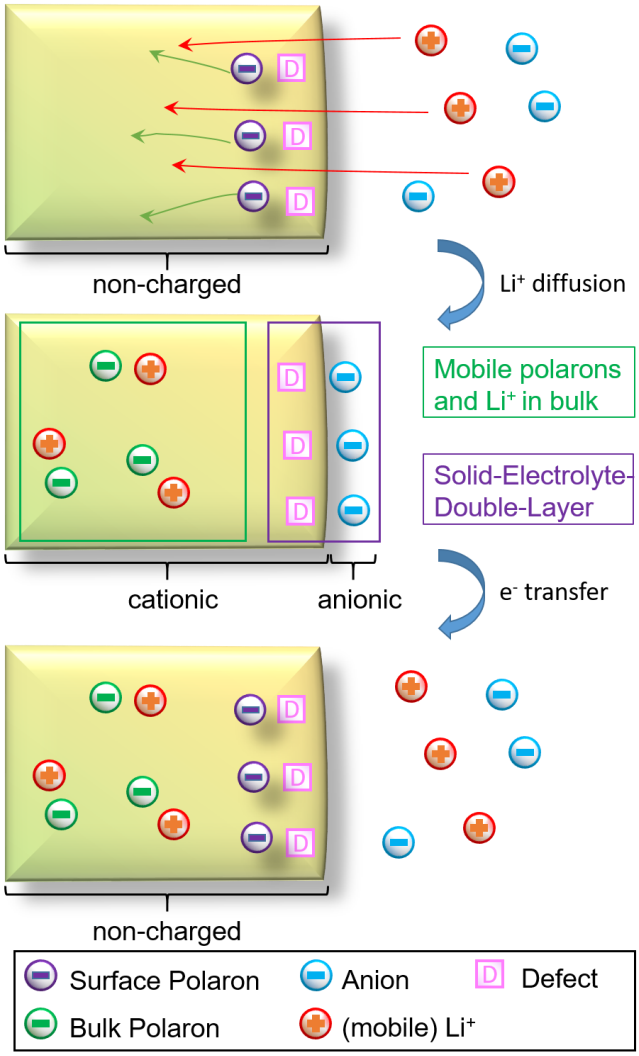

Figure 5: Surface defects with polarons enable lithium cations to diffuse into the bulk $Li_4Ti_5O_{12}$. It results a Solid-Electrolyte-Double-Layer to compensate the now positive charged particle due to the additional lithium cations in the bulk. A subsequent electron transfer to the particle restores a neutral $Li_{4+x}Ti_5O_{12}$ particle. X being the equivalent of intercalated lithium atoms.

Furthermore, we can conclude on a polaron based charge storage mechanism in LTO materials. It shows the surface with its defects and polarons does have a great influence on the electrochemical properties of the material. It can help to explain the observed high charging rates of very high surface LTO materials, with different capacitance contributions. In such systems it is possible that lithium diffusion into the material has happened before any electrons are transferred to the LTO. Then lithium diffusion into the material is not rate determining anymore, but the electron transfer is the rate determining step during the charging process. So when an electron is transferred to LTO, it compensates only a charge from the anion attached to the surface, making it a very fast process, like in a capacitor, enabling C/N >300.[16, 37] When on the other side the lithium diffusion process is limiting, due to a lower surface area and fewer polarons, the charging process is less effected by the “preequilibrium”, resulting in a more faradaic storage mechanism.

Summary

It was observed that LTO changes its bulk properties by contact with electrolyte in the form of different ^{7}Li NMR T_1 relaxation times. This effect is caused on the one hand by the polarons of surface or near-surface defects and on the other hand controlled by the cations of the electrolyte.
On the chemical level, an equilibrium between the liquid and solid phases can be concluded. Lithium ions from the electrolyte can diffuse together with the polarons from the surface into the bulk material. Thus - with respect to a charging process - the ion transport and the electron transport in LTO initially take place separately.
Consequently, the here presented work demonstrates the significant effect of surface defects and the associated polarons, on the properties of LTO as lithium storage materials. Hence, we believe the control of surface defects and polarons is an important tool to tune materials like LTO for battery or capacitor application.

Methods

All chemicals were purchased from Merck and stored under Argon atmosphere in a glovebox. Electrolytes and organic solvents were used without further purification. LTO nanopowder (<200nm) and lithium salts were stored for at least one week in a glovebox before use to remove potential water impurities.
For each experiment a Young-type NMR tube 150mg of LTO was filled and 1mL of electrolyte was added. The electrolyte consists of EC/DMC (1:1 weight ratio) mixture, having a 0M, 1M or 2M concentration of $LiPF_6$, LiTfl, LiTpb or NaTfl. The tube was shaken until a homogeneous slurry was obtained. Measurements were performed after 24h of settlement.
Static NMR experiments were performed on a Bruker Avance III HD 600 wide-bore spectrometer equipped with a gradient probe (Bruker PA BBO 600W2/S4 BB-H&F-D-05 DIFF). Saturation recovery experiments were used to determine ^7Li T_1 relaxation time. The number of accumulations was 8, using pi/2 pulses of 15µs at 50W. A series of up to 38 delays were used from 0.00001s to 1500s determine the buildup of the ^7Li signal.
Relaxation data was inverted using uniform penalty regularization,[38] which is a Tikhonov regularization algorithm in generalized form, in combination with a zero-crossing penalty to prevent sign changes in the calculated distribution that are not supported by the data.[25] Analyses were done with GNU Octave (version 4.0.3) using a home-written ILT function. For inversion, the 2D relaxation *vs.* spectral data was used. Thereby, only the relaxation dimension was inverted, but both dimensions were regularized. The resulting sensitivity gain from regularization along the non-inverted spectral dimension facilitated an improved resolution in the inverted relaxation dimension.[28] The regularization parameters have been chosen as detailed in.[39] The T_1 distribution was calculated at logarithmically spaced time constant values between 10^{-5} s and 10^8 s, with 10 points per decade. The upper limit was chosen to fit the bias, which occurs in saturation recovery experiments, into the distribution rather than as a single value with nominally infinite time constant. It was found empirically that this procedure produces more robust results in the case of multidimensional data sets.

Acknowledgements

Funding from the German Federal Ministry of Education and Research (BMBF project DESIREE, grant number 03SF0477A) is gratefully acknowledged.

Keywords: solid electrolyte interaction • lithium titanate • surface polarons • NMR • surface induced bulk change • non-faradaic process

ToC

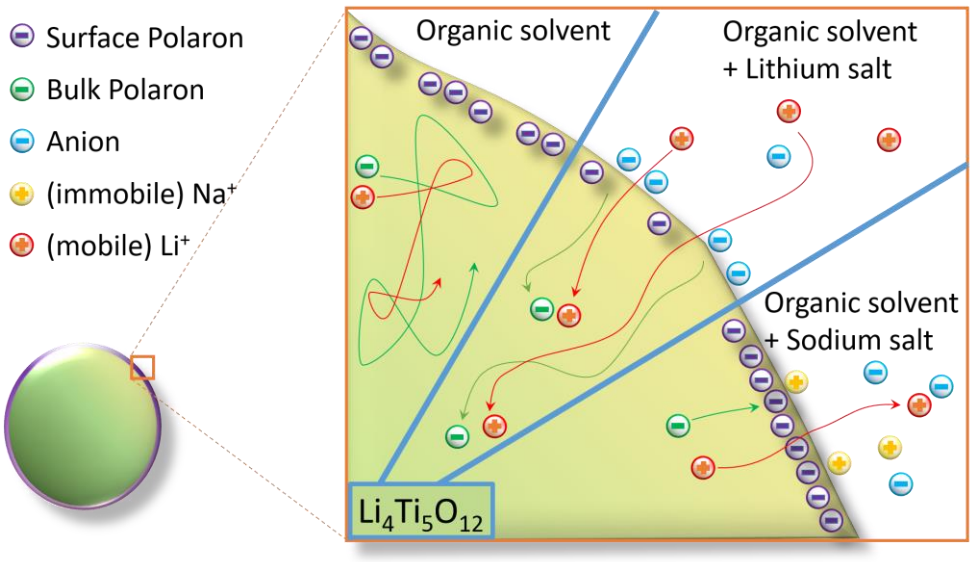

References

[1] I. Hadjipaschalis, A. Poullikkas, V. Efthimiou, *Renewable and Sustainable Energy Reviews* **2009**, *13*, 1513-1522.
[2] P. Simon, Y. Gogotsi, B. Dunn, *Science* **2014**, *343*, 1210-1211.
[3] M. Salanne, B. Rotenberg, K. Naoi, K. Kaneko, P. L. Taberna, C. P. Grey, B. Dunn, P. Simon, *Nature Energy* **2016**, *1*.
[4] M. R. Lukatskaya, B. Dunn, Y. Gogotsi, *Nature Communications* **2016**, *7*.
[5] N. Nitta, F. Wu, J. T. Lee, G. Yushin, *Materials Today* **2015**, *18*, 252-264.
[6] R. Marom, S. F. Amalraj, N. Leifer, D. Jacob, D. Aurbach, *Journal of Materials Chemistry* **2011**, *21*.
[7] Y. S. Hu, L. Kienle, Y. G. Guo, J. Maier, *Advanced Materials* **2006**, *18*, 1421-1426.
[8] J. Wang, J. Polleux, J. Lim, B. Dunn, *The Journal of Physical Chemistry C* **2007**, *111*, 14925-14931.
[9] D. P. Opra, S. V. Gnedenkov, S. L. Sinebryukhov, *Journal of Power Sources* **2019**, *442*.
[10] M. Madian, A. Eychmüller, L. Giebeler, *Batteries* **2018**, *4*.
[11] A. G. Dylla, G. Henkelman, K. J. Stevenson, *Accounts of Chemical Research* **2013**, *46*, 1104-1112.
[12] J. Lee, S. Adams, J. Maier, *Solid State Ionics* **2000**, *136-137*, 1261-1266.
[13] B. Zhao, R. Ran, M. Liu, Z. Shao, *Materials Science and Engineering: R: Reports* **2015**, *98*, 1-71.
[14] C. P. Sandhya, B. John, C. Gouri, *Ionics* **2014**, *20*, 601-620.
[15] W. Schmidt, P. Bottke, M. Sternad, P. Gollob, V. Hennige, M. Wilkening, *Chemistry of Materials* **2015**, *27*, 1740-1750.
[16] J. M. Feckl, K. Fominykh, M. Döblinger, D. Fattakhova-Rohlfing, T. Bein, *Angewandte Chemie* **2012**, *124*, 7577-7581.
[17] M. Wagemaker, E. R. H. van Eck, A. P. M. Kentgens, F. M. Mulder, *The Journal of Physical Chemistry B* **2008**, *113*, 224-230.
[18] M. Wagemaker, D. R. Simon, E. M. Kelder, J. Schoonman, C. Ringpfeil, U. Haake, D. Lützenkirchen-Hecht, R. Frahm, F. M. Mulder, *Advanced Materials* **2006**, *18*, 3169-3173.
[19] W. Schmidt, M. Wilkening, *Solid State Ionics* **2016**, *287*, 77-82.
[20] A. T. Brant, N. C. Giles, L. E. Halliburton, *Journal of Applied Physics* **2013**, *113*.
[21] W.-J. Yin, B. Wen, C. Zhou, A. Selloni, L.-M. Liu, *Surface Science Reports* **2018**, *73*, 58-82.
[22] M. Kick, C. Grosu, M. Schuderer, C. Scheurer, H. Oberhofer, *The Journal of Physical Chemistry Letters* **2020**, *11*, 2535-2540.
[23] N. A. Deskins, M. Dupuis, *Physical Review B* **2007**, *75*.
[24] M. Kick, C. Scheurer, H. Oberhofer, *The Journal of Chemical Physics* **2020**, *153*.
[25] J. Granwehr, P. J. Roberts, *Journal of Chemical Theory and Computation* **2012**, *8*, 3473-3482.
[26] M. C. Paulus, A. Paulus, P. P. M. Schleker, P. Jakes, R. A. Eichel, P. Heitjans, J. Granwehr, *Journal of Magnetic Resonance* **2019**, *303*, 57-66.
[27] M. C. Paulus, M. F. Graf, P. P. R. M. L. Harks, A. Paulus, P. P. M. Schleker, P. H. L. Notten, R. A. Eichel, J. Granwehr, *Journal of Magnetic Resonance* **2018**, *294*, 133-142.
[28] M. F. Graf, H. Tempel, S. S. Köcher, R. Schierholz, C. Scheurer, H. Kungl, R.-A. Eichel, J. Granwehr, *RSC Advances* **2017**, *7*, 25276-25284.
[29] Y.-Q. Song, H. Cho, T. Hopper, A. E. Pomerantz, P. Z. Sun, *The Journal of Chemical Physics* **2008**, *128*.
[30] T. Nordh, R. Younesi, D. Brandell, K. Edström, *Journal of Power Sources* **2015**, *294*, 173-179.
[31] M. Kitta, T. Akita, Y. Maeda, M. Kohyama, *Langmuir* **2012**, *28*, 12384-12392.
[32] R. Dedryvère, D. Foix, S. Franger, S. Patoux, L. Daniel, D. Gonbeau, *The Journal of Physical Chemistry C* **2010**, *114*, 10999-11008.
[33] Y.-B. He, M. Liu, Z.-D. Huang, B. Zhang, Y. Yu, B. Li, F. Kang, J.-K. Kim, *Journal of Power Sources* **2013**, *239*, 269-276.

[34] M.-S. Song, R.-H. Kim, S.-W. Baek, K.-S. Lee, K. Park, A. Benayad, *J. Mater. Chem. A* **2014**, *2*, 631-636.
[35] C. J. Jafta, C. A. Bridges, Y. Bai, L. Geng, B. P. Thapaliya, H. M. Meyer, R. Essehli, W. T. Heller, I. Belharouak, *ChemSusChem* **2020**, *13*, 3654-3661.
[36] D. Leanza, C. A. F. Vaz, I. Czekaj, P. Novák, M. El Kazzi, *Journal of Materials Chemistry A* **2018**, *6*, 3534-3542.
[37] K. Naoi, W. Naoi, S. Aoyagi, J.-i. Miyamoto, T. Kamino, *Accounts of Chemical Research* **2012**, *46*, 1075-1083.
[38] G. C. Borgia, R. J. S. Brown, P. Fantazzini, *Journal of Magnetic Resonance* **1998**, *132*, 65-77.
[39] S. Merz, P. Jakes, S. Taranenko, R.-A. Eichel, J. Granwehr, *Physical Chemistry Chemical Physics* **2019**, *21*, 17018-17028.